

Numerical Investigation of Performance of a Disc Shaped Branched Heat Exchanger

*Cihan Sezer^a, Kenan Kaya^b, Mahdi Tabatabaei Malazi^c, Enrico Sciubba^d,
Roberto Capata^e, and Hasan Alpay Heperkan^f*

^a Istanbul Aydin University, Istanbul, Turkey, cihansezer@aydin.edu.tr

^b Istanbul Aydin University, Istanbul, Turkey, kenankaya@aydin.edu.tr, CA

^c Istanbul Aydin University, Istanbul, Turkey, mahditabatabaei@aydin.edu.tr

^d Sapienza University of Rome, Rome, Italy, enrico.sciubba@gmail.com

^e Sapienza University of Rome, Rome, Italy, roberto.capata@uniroma1.it

^f Istanbul Aydin University, Istanbul, Turkey, hasanheperkan@aydin.edu.tr

Abstract:

This study investigates the heat transfer performance of a disc-shaped branched heat exchanger numerically. The numerical calculations have been conducted using the commercial computational fluid dynamics solver *ANSYS Fluent*, while three laminar and three turbulent cases are considered with Reynolds numbers of 100, 200 and 400 for the former; and 3000, 4000 and 6000 for the latter. Turbulence closure is achieved by employing the *k-eps* Realizable turbulence model, which uses Boussinesq approximation to model the eddy viscosity. The working fluid is water. Constant heat flux is applied at the bottom wall of the heat exchanger. The numerical method is validated by a previous experimental study. The heat transfer performance of the heat exchanger is evaluated by monitoring the temperatures at the outlet section, as well as the volume-averaged temperature of the solid part. It is observed that values of the heat transfer coefficient for the turbulent cases are much greater than that of the laminar case, whereas it is directly proportional with the Reynolds number, in general.

Keywords:

Disc shaped heat exchanger, Electronic device cooling, Computational fluid dynamics

1. Introduction

The purpose of this study is to carry on with the determination of the most effective configuration for a branching heat exchanger that uses water as the coolant fluid and implement any necessary improvements.

Capata and Gagliardi [1] investigated the performance of branched heat exchangers working with organic fluids. An automotive refrigerant called glycol was used in experiments at two different concentrations (50 and 100 %). An organic fluid has also been employed and examined for heat transmission. After completing all the tests, the numerous dimensionless parameters that characterize the heat exchange have been determined, and a comparison analysis has been performed, in order to determine and suggest the optimal configuration for the branched heat exchanger.

Reis [2] investigated constructal theory and its applications to a variety of domains, including engineering, natural living and inanimate systems, social structure, and economics. A constructal approach offers an integrated structure to guide the creation of flow architectures in systems with fluid flow. The relationship between of constructal law and the thermodynamic optimization strategy for minimizing entropy generation is described. The constructal law is an independent principle separate from the Second Law of Thermodynamics. In addition, the relationship between the constructal law and other fundamental concepts, including the Second Law, the principle of least action, and the principles of symmetry and invariance, is discussed.

Capata and Beyene [3] investigated three distinct compact branched heat exchangers by assessing the thermal efficiency and pressure drop of each device. A performance comparison of several refrigerant fluids improves the generality of the understanding of phenomena. To provide an average constant flow speed throughout the exchanger, the channels in the first arrangement have been built with different inner diameters. In the second, a constant flow Reynolds number has been maintained inside the channels. According to Bejan Constructal Theory, the final configuration is constructed using the constructal diameter variation. The results of multiple comparative tests have been assessed to find the ideal exchanger for each refrigerant based on the gathered data.

Asgari et al [4] considered the simulation of phase change material solidification in a heat exchanger with branch-shaped fins. The thermal conductivity of phase change materials is studied in relation to the impacts of branch-shaped fins with varying thicknesses and lengths. The results demonstrated that fins considerably

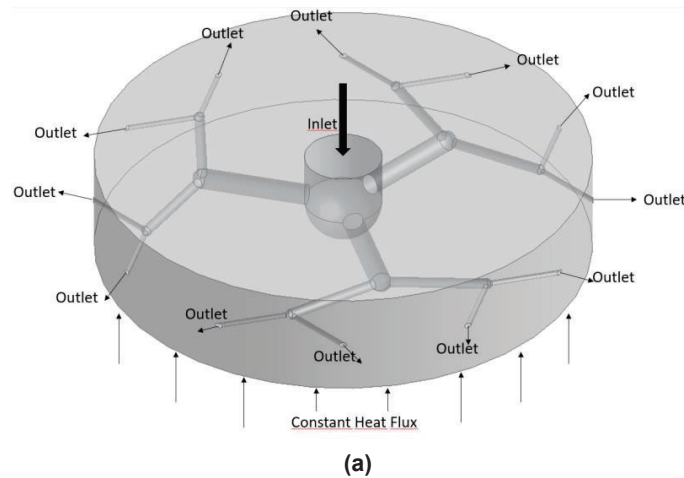
accelerate the solidification process, and simulation efficiency is maximized when thin, branch-shaped fins and nanoparticles with a volume fraction of 0.04 are utilized simultaneously.

Zhu and Jing [5] examined a numerical analysis of the thermal and melting performance of a horizontal latent heat storage unit with tree-like convergent fins. The paper presents a horizontal LHS unit embedded with branched tree-like convergent fins (BTCF) and statistically explores the influences of various geometric and structural characteristics of the BTCF. The results demonstrate that increasing N , m , and α values can efficiently enhance heat transfer between the fin and phase change material (PCM), speed up PCM melting, and increase energy storage.

Huang et al [6] studied the heat transfer improvement of a latent heat storage unit using gradient tree-shaped fins, both experimentally and numerically. They examine two new LHS units with tree-shaped uniform and gradient fins. The results indicate that tree-shaped fins promote heat diffusion from point to area, hence breaking the heat transport hysteresis in conventional LHS units and speeding the melting/solidification rate.

2. Numerical Method

This study investigates heat transfer characteristics in a disc shaped heat exchanger (Disc HEX), numerically. Steady, three-dimensional, and incompressible problem is modelled using commercial computational fluid dynamics (CFD) solver, *ANSYS Fluent*. Water as a heat transfer fluid for this study, enters disc heat exchanger through inlet section at temperature of 308 K with diameter of 22 mm which is located on the top of the disc heat exchanger. Diameter of branches are 5.9 mm, 2.9 mm, and 1.48 mm, respectively. Twelve outlets are located on sides of the disc and applied pressure outlet boundary condition, where static pressure is adjusted at zero gauge. Constant heat flux of 28294.212 W/m^2 is applied to the bottom of the disc for all cases. All surfaces of heat exchanger, except bottom surface where heat flux is applied, is considered adiabatic. Physical properties of water those of density, specific heat, heat conductivity and dynamic viscosity are assumed to be constant. Geometry description, branch definitions and boundary conditions are presented in Fig. 1 and Table 1.



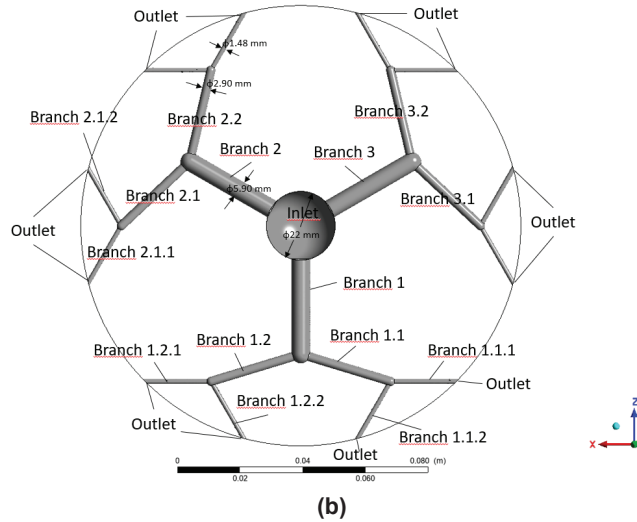


Figure 1. Geometry description and boundary conditions, (a) isometric view, (b) top view

An unstructured mesh with approximately 3.5 million elements is generated for numerical calculations (Fig. 2). Reynolds number is calculated considering inlet diameter and inlet velocity (Eq. 1). In numerical calculations, three laminar cases with Reynolds number of 100, 200 and 400, and three turbulent cases with Reynolds number of 3000, 4000 and 6000 are considered, respectively. For turbulent cases, k-ε Realizable turbulence model with Enhanced Wall Treatment is employed. Coupled algorithm is utilized for pressure-velocity coupling.

$$Re = \frac{\rho V_o D_o}{\mu} \tag{1}$$

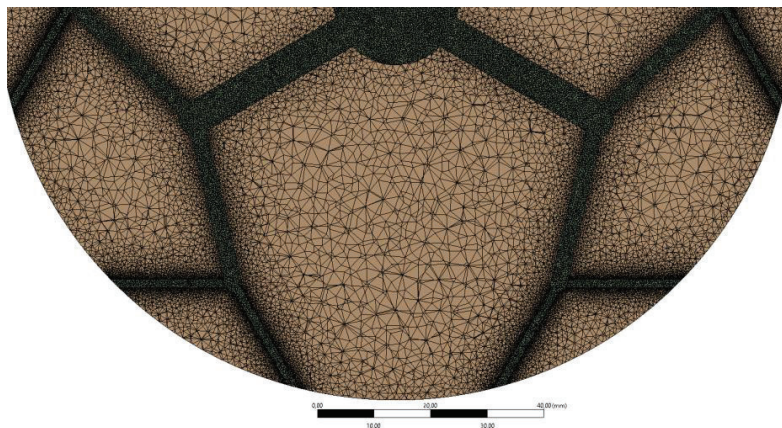


Figure 2. The numerical grid used in this study

Logarithmic mean temperature difference (ΔT_{lm}) is calculated according to Eq (2):

$$\Delta T_{lm} = \frac{(T_{wall,in} - T_{in}) - (T_{wall,out} - T_{out})}{\ln \frac{(T_{wall,in} - T_{in})}{(T_{wall,out} - T_{out})}} \tag{2}$$

Where, T_{in} and T_{out} refer to inlet and outlet temperatures of certain branch, while $T_{wall,in}$ and $T_{wall,out}$ refer to solid temperature near inlet and outlet sections. Heat flux is calculated through the following equation:

$$q = \frac{\dot{m}c_p(T_{out} - T_{in})}{A_s} \quad (3)$$

In Eq (3), A_s is heat transfer area, while \dot{m} and c_p are mass flow rate and specific heat. While mass flow rate is variable depending to Reynolds number, specific heat is assumed to be constant and 4182 J/kg K. Eventually, mean Nusselt number throughout each branch is calculated with Eq (4):

$$Nu_{m,i} = \frac{qD_i}{k \Delta T_{lm}} \quad (4)$$

Area-weighted average Nusselt number throughout whole disc for each case is calculated by Eq (5):

$$Nu_{m,ave} = \frac{\sum(A_s \times Nu_{m,i})}{\sum A_s} \quad (5)$$

3. Results and Discussion

This study is validated with a previous experimental work of Capata and Gagliardi [1]. Solution parameters used in the previous experimental work are employed in numerical calculations, and obtained results are compared. Validation parameters are given in Table 1, and compared results are presented in Table 2. Results of the numerical and experimental studies agree very well, while the absolute percentage error in the estimated values of temperature is 1.35 % for volume-averaged temperature of the heat exchanger, T_{solid} , whereas error is less than 0.5% for outlet fluid temperatures, T_{out} . Thus, the numerical model is validated to be used for further investigating heat transfer characteristics of the disc-shaped heat exchanger.

Table 1. Solution parameters

Refrigerant	Inlet velocity [m/s]	Reynolds number	Inlet Temperature [K]
Water	0.253	3267	304
	0.505	6534	309
	1.263	16336	312

Table 2. Comparison of experimental and numerical results

$T_{solid, exp}$ [K]	$T_{solid, num}$ [K]	Error %	$T_{out, exp}$ [K]	$T_{out, num}$ [K]	Error %
320.00	320.84	0.26	309.50	308.97	-0.17
318.80	320.26	0.46	311.3	311.31	0.003
315.00	319.25	1.35	312.80	312.81	0.003

Figure 3 illustrates the temperature distribution on the horizontal mid-plane of the heat exchanger. Accordingly, cooling effect increases with Reynolds number, while the maximum temperature decreases. It is also observed that fluid temperature increases with each branching. This increase in temperature can be attributed to the vortex formation in the junctions due to the impingement of fluid on the junction wall, as is seen in Fig. 4. Apparently, this is the primary factor increasing the heat transfer rate from solid walls to the fluid for all cases. Also, streamlines shown in Fig.4 indicate that higher values of velocity are observed in Branch 1.1.1 than those in Branch 1.1.2, since Branch 1.1.1 deviates from Branch 1.1 with a smaller angle than Branch 1.1.2 does. Temperature contours on the branch walls for Re=200 and 3000 (Fig. 5) are in accordance with those shown in Figs. 3b and 3d, where the wall temperature drops gradually as the fluid travels through the branches.

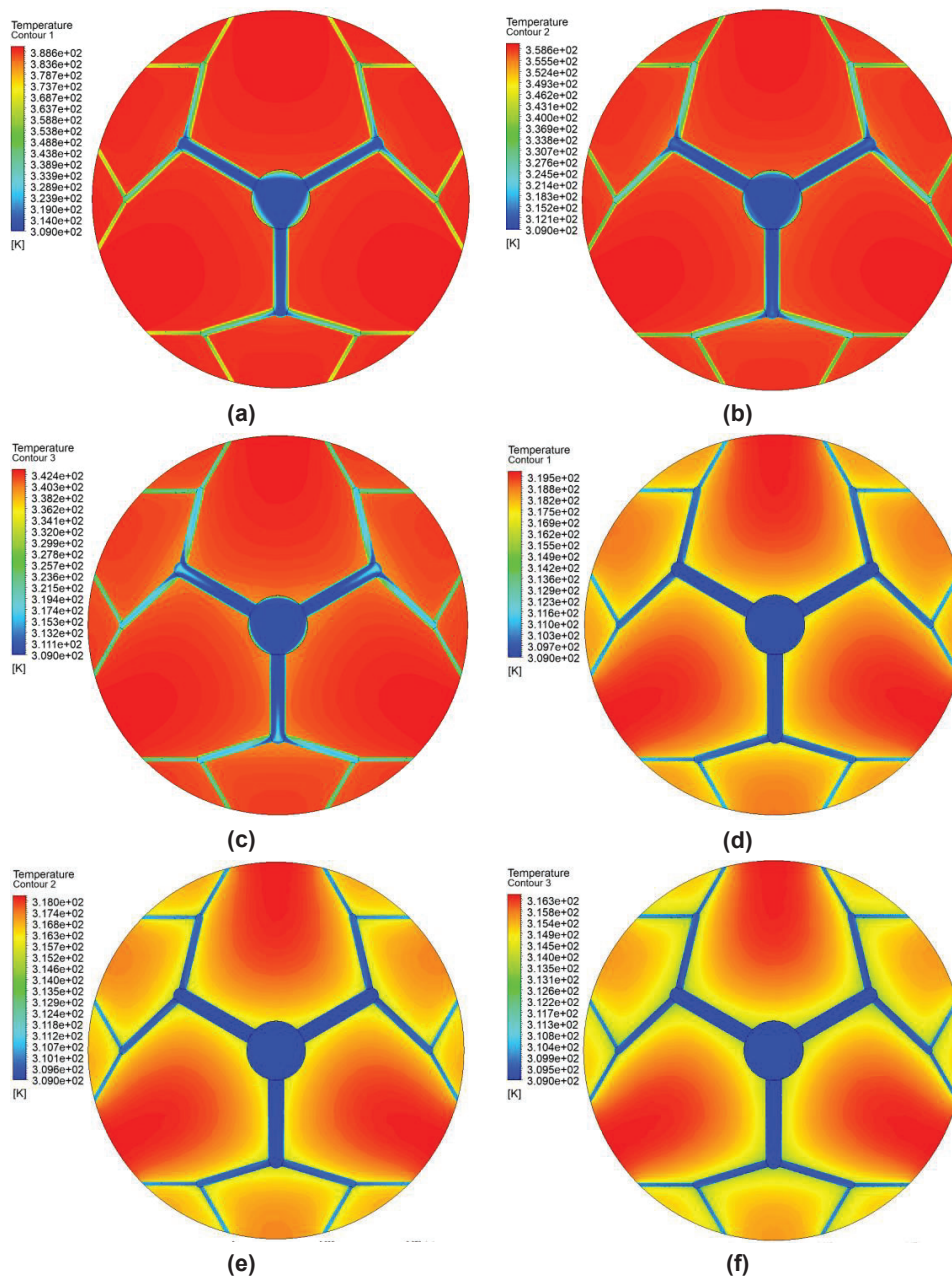


Figure 3. Temperature distribution on mid-plane of the disc heat exchanger for (a) $Re=100$, (b) $Re=200$, (c) $Re=400$, (d) $Re=3000$, (e) $Re=4000$, (f) $Re=6000$.

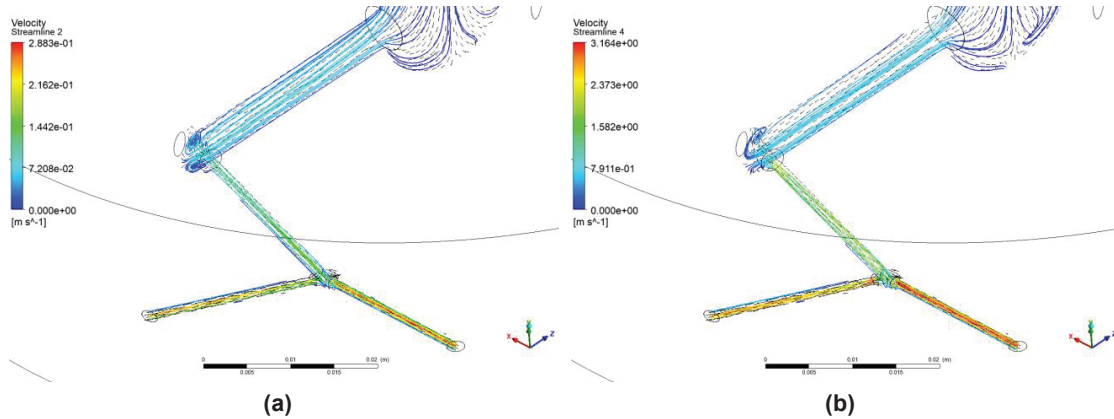


Figure 4. Streamlines and velocity vectors through branches for (a) $Re=200$ and (b) $Re=3000$

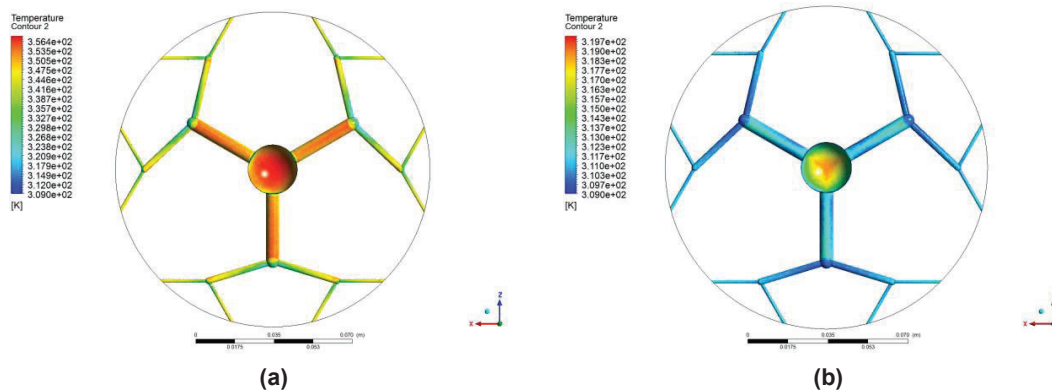


Figure 5. Temperature contours of the solid walls of the branches for (a) $Re=200$ and (b) $Re=3000$

Variation of calculated mean Nusselt number with branching is presented in Fig. 6 for each Reynolds number. It is interesting to note that mean Nusselt number in Branch 1.1.2 is higher than that in Branch 1.1.1 in case of laminar flow, while it is the other way around for turbulent cases (Fig. 6). One reason for such a difference might be the difference in temperature distribution as seen in Fig. 7. A horseshoe-like temperature profile is evident throughout the branches which is thought to be caused by the vortices generated at the junctions due to the impingement.

Figure 8 shows variation in area-weighted average Nusselt number ($Nu_{m,ave}$) for the whole disc heat exchanger with Reynolds number. Accordingly, there is a linear variation in Nusselt number which can be expressed by Eq. (6) with a normalized root-mean-square error (NRMSE) less than 2%:

$$Nu_{m,ave} = 0.216Re + 7.205 \quad (6)$$

Variation in average fluid outlet temperature and volume-averaged solid temperature of the heat exchanger is presented in Fig. 9. Both the average fluid temperature at outlet and volume-averaged solid temperature exhibits an exponential variation with the Reynolds number. It should be noted that in high Re number limit the average outlet temperature approaches the inlet fluid temperature, i. e. 308 K.

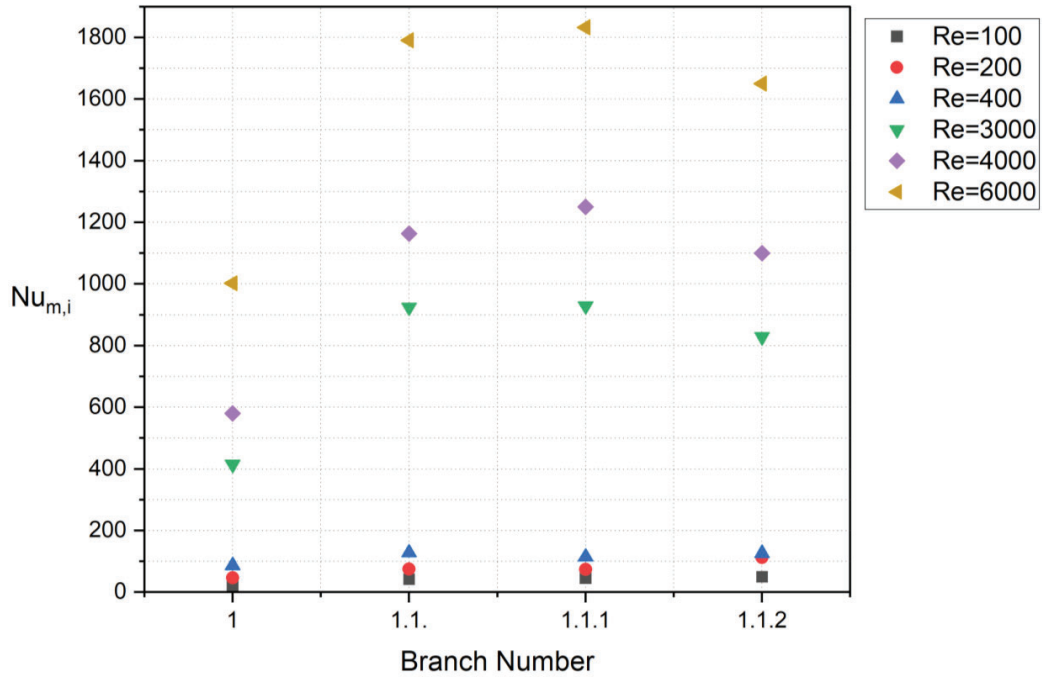


Figure 6. Variation of mean Nusselt number with branching

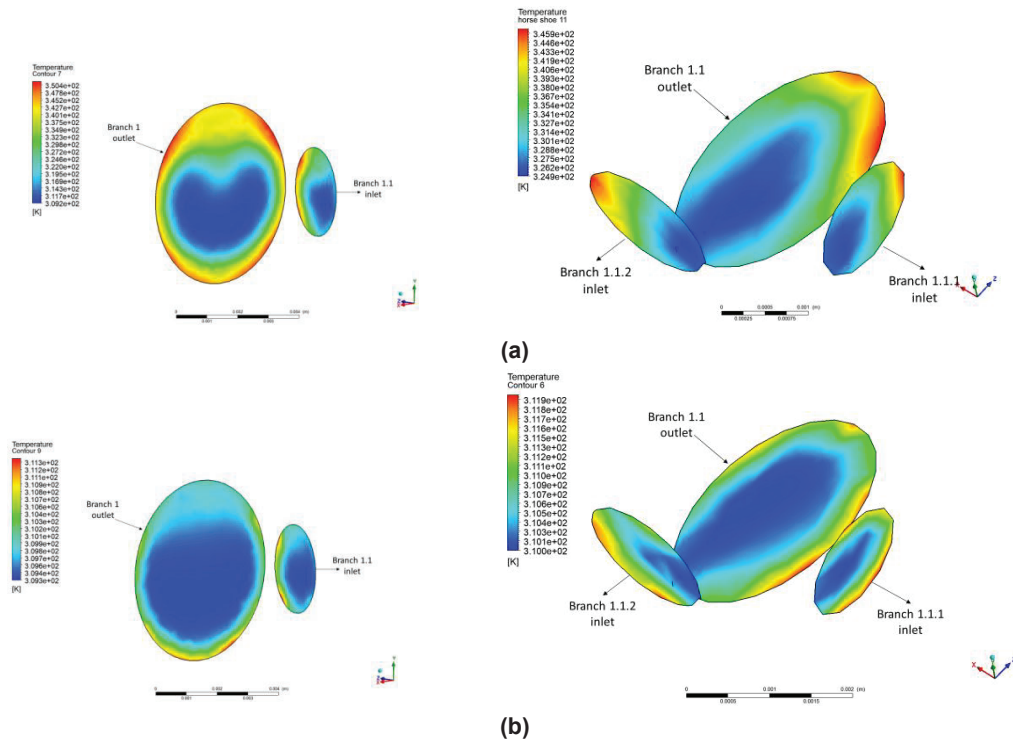


Figure 7. Temperature contours on inlet and outlet planes of branches for (a) $Re=200$ and (b) $Re=3000$

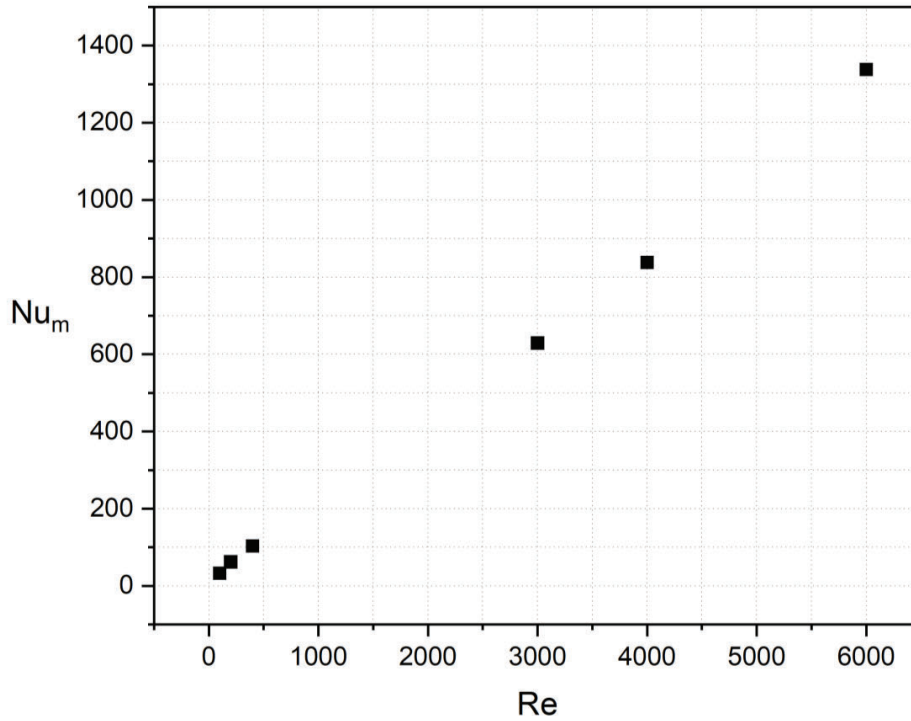


Figure 8. Variation in area weighted average Nusselt number for the whole disc heat exchanger with Reynolds number

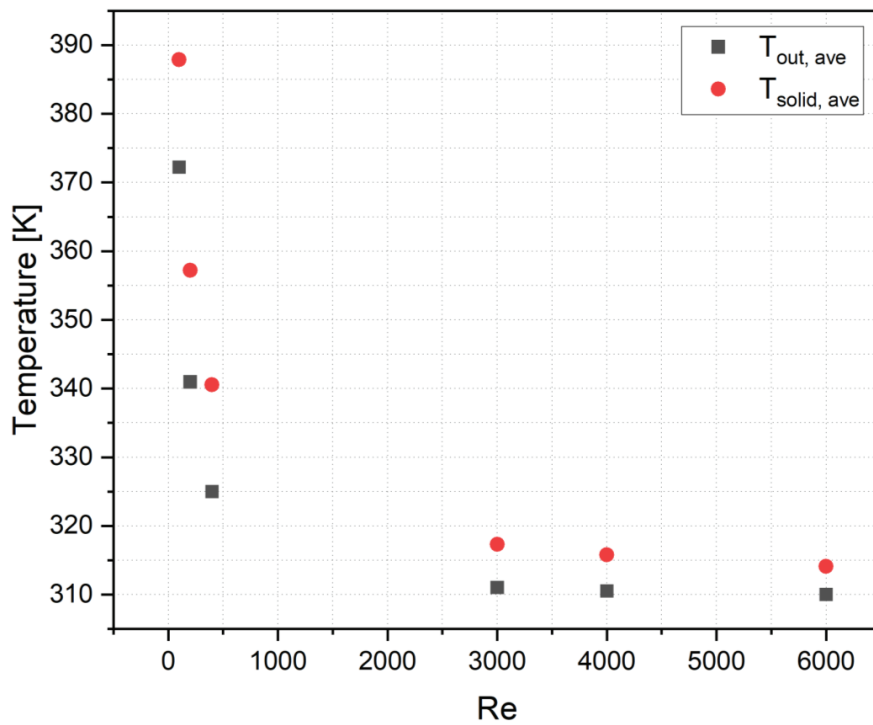


Figure 9. Variation in average fluid outlet temperature and volume-averaged solid temperature with Reynolds number

4. Conclusion

In this study, heat transfer characteristics of a disc-shaped branched heat exchanger is investigated for laminar and turbulent cases for Reynolds numbers of $Re = 100, 200, 400, 3000, 4000$ and 6000 . The flow pattern and its effect on the heat transfer coefficient is discussed. According to the numerical results, mean Nusselt number for a given branch and the whole disc increases with the Reynolds number. The variation of the average Nusselt number for the whole disc with the Reynolds number is almost linear, a first order polynomial expression is offered which yields the average Nusselt number corresponding to a given Reynolds number with a maximum normalized root mean square error of less than 2%, for $100 \leq Re \leq 6000$. Extremely high values for volume-averaged solid temperatures are calculated for cases of relatively lower Reynolds number, which may exceed the design temperatures of device to be cooled. On the contrary, volume-averaged solid temperature of the heat exchanger approaches the inlet temperature of the coolant at high Reynolds numbers.

It is observed that the most significant factor affecting heat transfer coefficient of the disc-shaped heat exchanger is fluid impingement on the walls in junctions. This implies that a design allowing more effective impingement may provide higher heat transfer characteristics. However, although pressure losses are not considered in this study, a trade-off should be made between pressure loss and increase in heat transfer coefficient.

Nomenclature

A_s surface area m^2

c_p specific heat, $J/(kg K)$

D diameter m

k heat conductivity $W/(m K)$

\dot{m} mass flow rate, kg/s

Nu_m average Nusselt number

T_{in} inlet temperature K

T_{out} outlet temperature K

$T_{out,ave}$ average outlet temperature K

$T_{solid,ave}$ volume-averaged solid temperature K

$T_{wall,in}$ solid temperature near inlet K

$T_{wall,out}$ solid temperature near outlet K

ΔT_{lm} logarithmic mean temperature difference K

q heat flux W/m^2

V velocity m/s

ρ density kg/m^3

μ dynamic viscosity $kg/(m s)$

References

- [1] Capata, R., Gagliardi L., Experimental investigation on the Reynolds dependence of the performance of branched heat exchangers working with organic fluids. *Int. J. Heat Mass Transf.* 2019; 140: 129-138.
- [2] Reis, A. H., Constructal theory: from engineering to physics, and how flow systems develop shape and structure. *Appl. Mech. Rev.* 2006; 59(5): 269–282.
- [3] Capata, R., Beyene, A., Experimental evaluation of three different configurations of constructal disc-shaped heat exchangers. *Int. J. Heat Mass Transf.* 2017; 115: 92–101.
- [4] Asgari, M., Javidan, M., Nozari, M., Asgari, A., Ganji, D.D., Simulation of solidification process of phase change materials in a heat exchanger using branch-shaped fins. *Case Studies in Thermal Engineering.* 2021; 25: 100835.
- [5] Zhu, R., Jing, D., Numerical study on thermal and melting performances of a horizontal latent heat storage unit with branched tree-like convergent fins. *Journal of Energy Storage.* 2023, 62: 106889.
- [6] Huang, Y., Cao, D., Sun, D., Liu, X., Experimental and numerical studies on the heat transfer improvement of a latent heat storage unit using gradient tree-shaped fins. *Int. J. Heat Mass Transf.* 2022; 182: 121920.